Available online at www.sciencedirect.com

ScienceDirect

Procedia Engineering 197 (2017) 89 – 98

Procedia Engineering

www.elsevier.com/locate/procedia

DYMAT 23rd Technical Meeting

Dynamic Fracture of Ductile Materials

Tensile test of a HSLA steel at high strain rates with two different SHTB facilities

G. Mirone [a*], R. Barbagallo [a], E. Cadoni [b]

[a]*DICAR, University of Catania, Viale A. Doria 6, 95125 Catania - Italy*
[b]*DynaMat Laboratory, University of Applied Sciences of Southern Switzerland, CH-6952 Canobbio, Switzerland*

Abstract

The dynamic stress-strain curves obtained by Hopkinson bar testing can be subjected to a variety of possible approximations including hardware-based issues and/or accuracy reductions due to the procedures for the analysis and the post-processing of the experimental data. In order to highlight the possible occurrence of such approximations and to eventually assess their magnitude, quasi-static and dynamic tensile tests have been carried out on a 3*8MnSiVS6* steel, adopting two different Split Hopkinson Tensile Bars (SHTB) adopting different mechanical solutions for the input bars clamping / releasing systems. High speed video acquisition with frames extraction and image analysis delivered the evolving specimen geometry and its dimensions all over the test duration. Slightly different procedures are also adopted for the analysis of the raw experimental data leading to the relationships between stress, strain and strain rate for each test. The stress–strain curves and the strain rate–strain curves are derived from both series of experiments according to the engineering approach and to the true approach, the latter being obtained according to different hypotheses for the post-necking evolution of the true curve. High speed camera helped in measuring via image analysis the current evolving area of the neck section allowing to derive the true strain, true strain rate and true stress to be compared to the similar variables determined from the strain gauges on the bars.

Peer-review under responsibility of the scientific committee of the International Conference on Dynamic Fracture of Ductile Materials

Keywords: Split Hopkinson Tensile Bar, high strain rate, true stress-strain, clamping.

* Corresponding author. Tel.: +39 095 7382418
E-mail address: gmmirone@diim.unict.it

Peer-review under responsibility of the scientific committee of the International Conference on Dynamic Fracture of Ductile Materials
doi:10.1016/j.proeng.2017.08.085

1. Introduction

The Split Hopkinson Tension Bar (SHTB) is used for tests with strain-rates greater than 10^2 s^{-1} where it is essential not to interfere with the propagation of waves.
The main architectures in the literature for generating tensile waves on specimens are based on:

- Interposition of a sleeve between the bars of a standard compression machine, parallel to the specimen, so that the tension is generated by the wave reflections at the interfaces between the bars and the sleeve.
- Tubular striker coaxial to the input bar and travelling along it, so that the tension is generated by the impact of the striker hitting a stopper at the free end of the input bar.
- Tension preload of a segment of the input bar and its sudden release, originating a tension wave travelling toward the specimen according to the Albertini-Montagnani (1974) [4] or Staab-Gilat (1990) approaches.

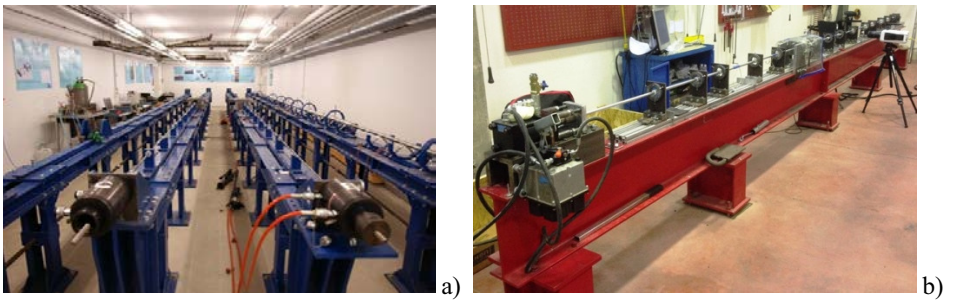

Fig. 1. SHTB facilities adopted at SUPSI (a) and at UNICT (b), respectively

The facilities analysed (see Fig. 1) in this work are of the third type and are installed at the DynaMat Laboratory of the University of Applied Sciences of Southern Switzerland (SUPSI) and at the Laboratory of mechanics of the University of Catania (UNICT). In such group, there are different typical solutions for blocking a section of the pre-tensioned input bar, like those of nutcracker-like clamp tightened by a suspended actuator (Fig. 2), from which that at UNICT is derived and the Theta clamp which is used at the SUPSI.

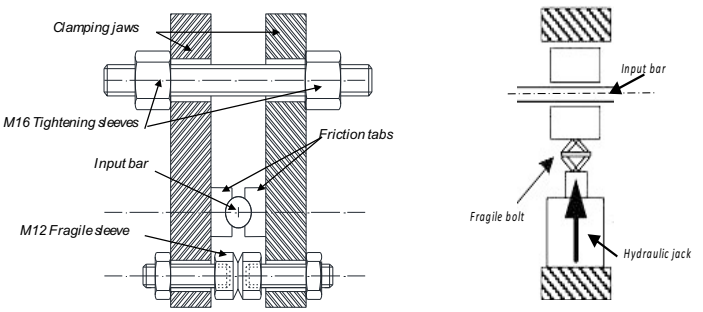

Fig. 2. Clamp architectures: left) UNICT; right) SUPSI

The overall setup of the SHTB and, in particular, the clamping system, are crucial for the generated incident wave and its rise time. Too low rise times can induce equilibrium and dispersion problems while too high rise times delay the strain wave plateau and do not allow to

ensure a nearly constant strain rate to the specimen all over test, also depending on the specimen geometry.

This work compares the experimental outcome of two different SHTB devices for dynamic tensile tests at high strain rate, respectively available at the DynaMat laboratory (SUPSI) and at the Laboratory of mechanics (UNICT).

The engineering stress-strain curves are poorly representative of the real material behavior and greatly affected by the specimen geometry, as also discussed in Mirone et al. [1], while the true curves are virtually identical to the flow stress up to the necking onset. Then the comparison of experimental results is done in terms of the true-stress-true strain curves, which, in principle, require the knowledge of the current minimum diameter of the specimen. Indeed, the true curves at UniCT are based on diameter measurements via high-speed camera and image analysis.

Instead, the true curve from SUPSI experiments are based on the mathematical transformation of the engineering curves in the true ones, only valid up to the necking onset for specimens with slenderness above a minimum threshold, and on the evaluation of true stress and true strain at failure via cross section measurements on the broken specimen. The unknown true data between necking and failure are approximated by a linear segment connecting the above data.

Also the post-necking transformation of the true curves for estimating the flow curves is performed according to slightly different procedures; the UNICT curves are obtained by the material-independent MLR polynomial; while the SUPSI ones are calculated by the Bridgman correction of the last point joined to the same linear approximation adopted for the true curves.

Then this comparison highlights the purely “equipment-based” differences between the two series of experimental data on one side, as well as the post-processing-based differences due to the procedures for determining the current cross section and the post-necking transformation of the true curve in to an estimation of the flow curve, on the other side.

2. Experiments

2.1. Material and specimens

Forging grade steel *38MnSiVS6* is a micro alloyed steel mainly used in the automotive industry to make crankshafts thanks to its mechanical properties, i.e. high tensile strength, good value of impact resistance and relative lightness.

The chemical composition is given in Table 1, the mechanical properties are the following: Elastic modulus E=190GPa, density ρ=7829kg/m^3; yield stress $R_{0.2}$= 645MPa, R_m=930MPa, uniform deformation ε_u=7.5%. and thermal properties of the *38MnSiVS6* obtained by Korchynsky and Paule [2] are shown in Table 2.

Table 1 Chemical composition of 38MnSiVS6

Material	C	S	Cr	Ni	Mn	Si	V	Fe
38MnSiVS6	0.4	0.05	0.20	0.02	1.43	0.24	0.10	Bal.

Table 2 Thermal properties of 38MnSiVS6 [2]

Material Property	SI base units
Thermal expansion	1.21e-5 K^{-1}
Thermal conductivity	34.2 W / mK
Specific heat capacity	517 J / kg·K

All the specimens tested in this work, both statically and dynamically, were round specimen having diameter of 3mm and gauge length of 5mm [5,10].

2.2. SUPSI SHTB equipment and characterization procedure

In the DynaMat laboratory in Lugano there are four Modified Hopkinson Bars (MHB) developed following the studies of Albertini and Montagnani [3, 4] (see Fig. 1a). By means of such facilities, it is possible to execute tensile, compression and shear tests on polymeric [11] and metal [12] specimens also at high temperature thanks to an Ambrell compact EASYHEAT induction water-cooled heating system [13]. This type of equipment allows performing tests at strain rates varying from 100 to 2,000 s^{-1}.

The SHTB consists of a pre-tensioned bar (substituting the projectile of the classic Hopkinson bar) which has as solid continuation the input bar, followed by the output bar and the specimen inserted between the two lasts bars as shown in Fig. 3. In particular, the used equipment is composed by high strength steel bars with a diameter of 10mm. The input bar length is 9m, of which 6m pre-tensioned, while the output bar length is 6m. Thanks to 6m of pre-tensioned bar, it is possible to generate 2.4ms tensile waves able to lead to fracture the specimen also at relative low strain rates.

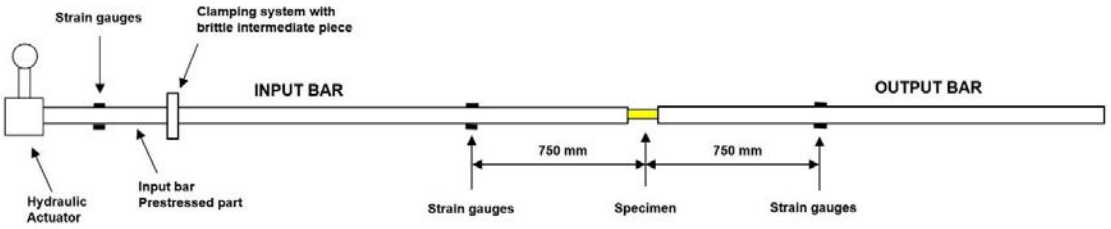

Fig. 3. SUPSI SHTB Scheme

The SHTB functioning is based on storing a certain amount of elastic mechanical energy in the pre-tensioned bar which is blocked by a brittle intermediate piece, while the other end is pulled by means of a hydraulic actuator. The originality of this SHTB is in the blocking device, which permit a very rapid load ramp in the order of 30 μs. The brittle intermediate piece, called also the "theta clamp", because resembling this Greek alphabet letter [5], is shown in Fig. 4 and consists of a quadratic parallelogram whose sides are kept together by four supporting pieces placed at the vertex of the parallelogram. One of those supporting pieces is in contact with a hydraulic actuator and the diagonally opposite piece is in contact with the end section of the pre-tensioned bar; the two other pieces are hold together by a notched brittle bolt.

During the phase of static pulling of the pre-tensioned bar, the hydraulic actuator acting on one vertex of the parallelogram exerts a transversal force, passing through the sides of the parallelogram and through the notched brittle bolt, on the end section of the pre-tensioned bar blocking it by friction.

After the static pre-tensioning phase for elastic energy storage has been completed, the transversal hydraulic actuator increases the force passing through the parallelogram sides and the notched bolt until the notched bolt fractures in a brittle manner, provoking the sudden failure of the parallelogram. The controlled failure of the parallelogram is the key factor for assuring that the end section of the pre-tensioned bar is very suddenly left free as needed for the generation of a tension pulse having the very short rise time of about 30μs. The end section of the pre-tensioned bar is left free in a clean manner without receiving unwished transversal bending pulses and therefore assuring that the tension wave propagation toward the specimen along the incident bar is an elastic plane wave without bending components. The obvious importance of a well-constructed and operating theta clamp to insure the scientific validity of the SHTB highlights why this very original design was patented [3,4].

Fig. 4. SUPSI Theta clamp

As it is possible to see in the Fig. 3, for the acquisition of the signals there are two strain gauge stations placed in the input and in the output bars, both at 750 mm from the specimen. By means of the first one, it is possible to read the bar deformation caused by the incident wave ε_I and by the reflected wave ε_R, which is related to the deformation of the specimen; the distance from the specimen was chosen to clearly distinguish the incident wave from the reflected one. The second station is used to record the transmitted wave that represent the resistance of the specimen. There is also a third strain gage station placed in the pre-tensioned bar to control the preload. All the signals are recorded with a HBM-GEN2i, characterized by an acquisition rate of 1 Msample/s.
Based on the record of ε_I, ε_R and ε_T and considering the basic constitutive equations of the input and output elastic bar and the one-dimensional wave propagation theory, it is possible to calculate the engineering stress, strain and strain-rate (eq. 1-3)

$$\sigma_{eng}(t) = E_0 \frac{A_0}{A} \varepsilon_T(t) \tag{1}$$

$$\varepsilon_{eng} = -\frac{2C_0}{L} \int \varepsilon_R(t)\, dt \tag{2}$$

$$\dot{\varepsilon_{eng}} = -\frac{2C_0}{L} \varepsilon_R(t) \tag{3}$$

where: E_0 is the elastic modulus of the bars; A_0 is the cross-section area of the bars; A is the specimen cross-section area; L is the specimen length; C_0 is the sound velocity in the bar.

Fracture strain is obtained by microscopy measurement as the reduction of the area at fracture:

$$RA[\%] = \frac{(A_0 - A_F)}{A_0} \tag{4}$$

where A_0 is the initial cross-section area and A_F is the cross-section area of the fracture. The engineering stress vs. strain curves in tension are transformed in true stress vs. true strain curves until the necking onset by means of the following well-known relationships:

$$\sigma_{true} = \sigma_{\mathrm{Eng}}(1 + \varepsilon_{Eng}) \tag{5}$$

$$\varepsilon_{true} = \ln(1 + \varepsilon_{Eng}) \tag{6}$$

After the necking onset, it is not possible to use these relationships anymore but, analysing by means of an optical microscope the broken specimen, it is possible to evaluate the fracture area that, coupled with the fracture force, gives us the last point of the true curve. Linking the necking

point to this last point, we obtain the complete true curve.

In order to compare the results of the dynamic tests carried out at the DynaMat laboratory with the results obtained at the UNICT, in Catania a preliminary study of the experimental data obtained at the DynaMat has been carried out. In particular, the strain gauge signals and the videos of the tests, recorded with a high-speed camera, have been analysed in order to obtain the true curves as explained afterwards.

2.3. UNICT SHTB equipment and characterization procedure

The SHTB installed at the Mechanics laboratory of the University of Catania (see Fig. 1b) is based on 4.5 and 3 meters long input and output bars, respectively, both with 16 mm diameter and made of Al7075 alloy. As it is possible to see in the Fig. 5, the strain gauge stations are respectively 450 mm and 550 mm from the specimen. The signals of these strain gauge stations and of another one installed in the pre-tensioned bar are recorded with a Dewetron DEWE-30-16 Signal Conditioning Chassis with an acquisition rate of 3 Msample/s.

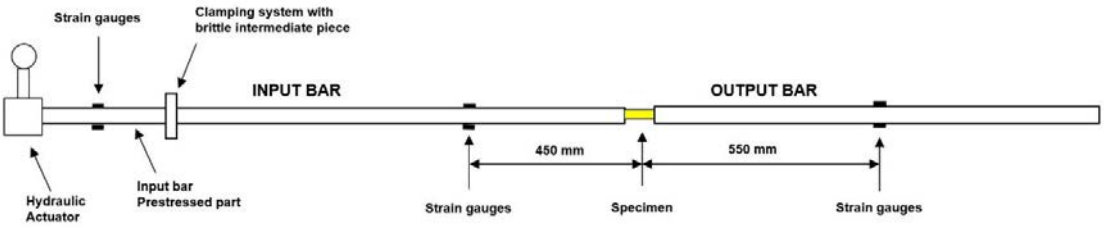

Fig. 5. UNICT MHB Scheme

The main difference between the SUPSI's and the UNICT's setups is the clamping device. The UNICT's clamping device is shown in Fig. 6. It consists of two vertical jaws of 7075 Al alloy pressing pair of friction tabs against the input bar; a notched brittle sleeve passes through holes at the lower side of the jaws, while a threaded bar, passing through larger holes on the upper side of the clamps, is manually tightened and acts as the actuator. The architecture is that of a nutcracker-like leverage, where significant force variations can be obtained by simply varying the ratio of the relevant distances.

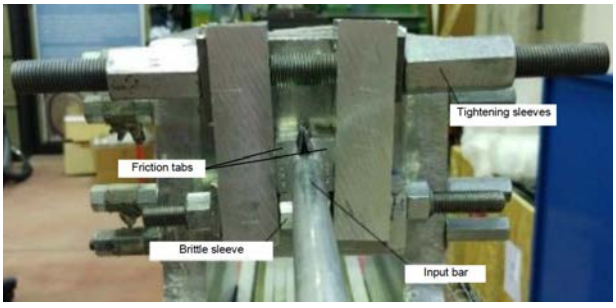

Fig. 6. UNICT nutcracker-like clamp

Firstly, the threaded bar is tightened enough to hold the input bar, by friction, and allowing its pre-tensioning; then the top screw is tightened up to the limit traction load of the brittle intermediate piece in order to break it and suddenly release the elastic energy stored in the pre-tensioned bar. With this setup it is possible to obtain rise times of the incident wave of about

100μs, although downsizing and inertia reduction should allow significant reductions of the rise time. A comparison of two incident waves from the release systems at SUPSI and at UNICT is reported in Fig. 8

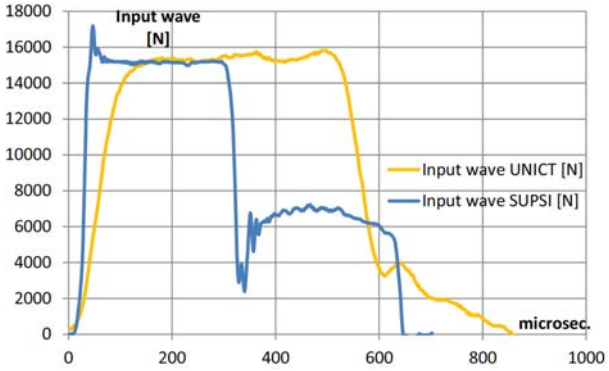

Fig. 7. Incident waves from SUPSI and UNICT experiments

The true curves are obtained from the strain gauge measurements coupled to the high-speed videos. The current minimum cross section is obtained by image analysis of frames extracted from the fast camera capture and the current load is obtained from standard strain gauge-based readings typical of the SHTB technique.
Both data are synchronized each other by coupling together the frame from the camera clip at fracture (the frame before the specimen is broken in two halves) and the corresponding reading of the transmitted wave (the reading at which the transmitted wave falls), both easily recognizable; then, at desired time intervals, other frames (current specimen cross section) and strain gauge readings (specimen load) are selected, by simply going backward of the same time amount, based on the knowledge of the corresponding acquisition rates.

3. Results and discussion

The test programme at high strain-rate performed at the SUPSI concerned the obtaining of the true stress versus true strain curves in tension at various nominal engineering strain rates (250 s^{-1}, 500 s^{-1}, 600 s^{-1}, 1000 s^{-1}) at the room temperature and also at high temperature. The subsequent test programme performed in Catania concerned high strain rate tests at room temperature and at different input bar preloads (20.8 kN to 26 kN).

Considering only the room temperature tests, three representative SUPSI tests and four representative UNICT tests at different measured effective nominal strain rate have been chosen to compare the different characterization procedures and hardware (Table 3).

Table 3 Specimens and nominal strain rates

Specimen	Measured nominal strain rate [s^{-1}]
SUPSI 23	330
SUPSI 24	530
SUPSI 25	1110
UNICT 31	800
UNICT 32	800
UNICT 33	500
UNICT 34	600

First, a comparison between the different characterization techniques has been done by considering the specimens tested at the SUPSI. In Fig. 8, the true curves obtained analysing the high frame rate videos (CAMERA specimens) are compared with the true curves obtained from

the engineering curve with eq. 5-6 until the necking onset and linking this last point with the point obtained coupling the area of the broken specimen observed by means of optical microscope and the fracture force (FIN DIAM specimens).

The true curves at failure from high-speed camera resulted to be 8% greater than those determined with the Final Diameter technique. This approximation might be due to the difference between the actual diameter at incipient failure and the "post-mortem" diameter measured by optical microscope.

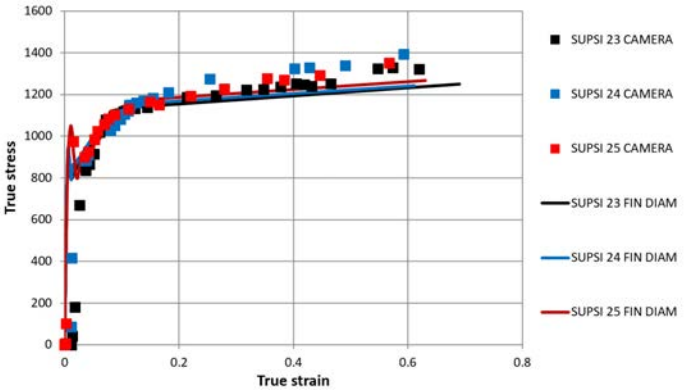

Fig. 8. SUPSI true curves comparison – CAMERA vs. Final Diameter method

In fact, when the fracture is not yet fully propagated and the specimen is still loaded, the shape and size of the cross section is reasonably different from the same cross section after the fracture is completely propagated and the specimen, unloaded, is separated in two halves: this is because the fracture propagation is not immediate and consists of further specimen distortion at the local scale, which may affect the Final Diameter technique, and also because as the specimen is still loaded is undergoes some elastic Poisson-induced shrinking.

Another worth noting point common to both series of experiments, is that, despite very different nominal strain rates, the true curves obtained for the different tests are almost indistinguishable from each other, no matter which characterization technique is used.

In principle, the above difference might be due to an unknown mix of purely-experimental response between the two facilities and post-processing techniques referring to the cross-section measurements.

Then, for separately assessing the differences generated by the two causes above, the diameter measurements from fast camera have been carried out also for the tests at SUPSI and the comparison of the true curves from UNICT and from SUPSI, obtained by the same experimental technique, are compared in Fig. 9.

As it is clearly visible, all the true curves are included in a narrow band showing the overall equivalence of the two facilities and confirming that this material is either not affected by the strain rate effect or the strain rate effect is small enough to be compared to the scattering of the experimental data. One more evidence from Fig. 9 is that the true strains at failure slightly differ each other being about 0.8 according to the UNICT tests, 0.6 to SUPSI Camera tests and 0.65 according to the "fully" SUPSI procedure.

By combining the information from Fig. 8 and Fig. 9, the overall stress difference between the "fully" SUPSI true curves (obtained from engineering curves until the necking onset + Final Diameter) and the UNICT ones (from camera) is close to +8% at the necking onset and -13% at failure.

The obtained true stress versus true strain curves are equal to the flow curve until the necking onset. After this point, the strain localization implies that the flow curve diverges from the true

curve, which is no more representative of homogeneous mechanical properties of the materials. The most known post-necking correction used to obtain the flow curve from the true curve is due to Bridgman [6], although the reverse engineering approach based on finite elements and on the simple engineering data is also diffused in the literature. A faster procedure was introduced for the quasi-static necking correction in Mirone [7], transforming the post-necking σ_{True} into an estimation of σ_{eq} by a simple corrective function MLR, available independently of the material and capable of delivering an accuracy around 3%.

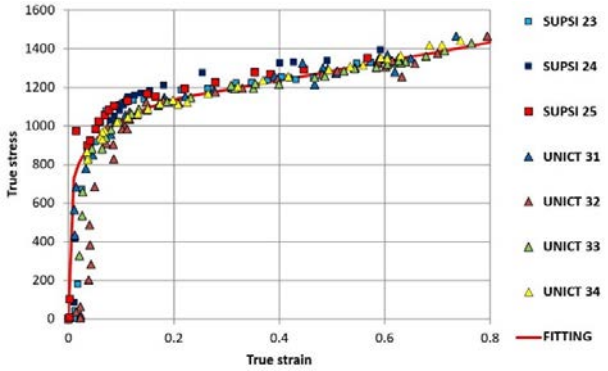

Fig. 9. True curves from camera comparison – SUPSI vs UNICT

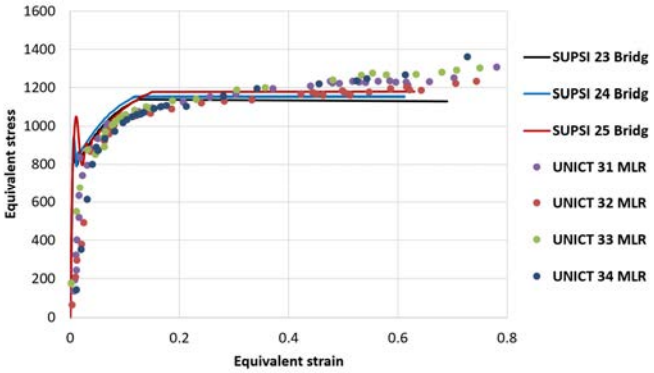

Fig. 10. SUPSI vs UNICT equivalent curves comparison

The Bridgman approach can be applied all over the post-necking phase but it is often used only for the last point of the true curve because it is possible to have a high-resolution image of the broken specimen with a standard camera. It is important to underline that this last approach includes further approximations due to the difference between the actual fracture diameter and the one that is measured after a certain amount of time after the fracture as explained before. The application of such approach is laborious and not perfectly objective, therefore to apply it to low-resolution images obtained with a high frame rate camera in order to obtain further points between the necking onset and the fracture of the specimen could be difficult and uncertain. On the other hand, the usage of the MLR function is straightforward and can be done without the optical analysis of the images.

In Fig. 10 is shown the comparison between the equivalent stress – equivalent strain curves obtained with the complete methodology at the SUPSI (true curve obtained from engineering curve until the necking onset + Final Diameter + Bridgman correction) and at the UNICT (true curve from camera + MLR). As it is possible to see in such figure, the stress differences between the SUPSI and UNICT true curves are reflected also in these final equivalent curves, with SUPSI

curves at failure lower than the UNICT ones of about 10%.

4. Conclusion

The aim of this work was the comparison between the characterization techniques and the experimental results of two different SHTB facilities for dynamic tensile tests at high strain rate. The two SHTB devices considered, one developed at the DynaMat laboratory and the other at the Laboratory of Mechanics at the University of Catania, were described focusing on the substantial differences such as the setup, the blocking device, the achieved rise time and the tests carried out. The experimental results from the DynaMat tests were collected and, according to the standard theory of the Hopkinson bar based on strain gauge measurements, engineering curves were found; then, the true curves were obtained from such curves until the necking onset and by diameters measurement on the broken specimens afterwards.

A further analysis of the SUPSI test results was then made at Mechanics laboratory of UNICT before carrying out further tests on similar specimen at similar strain rates; such preliminary analysis was based on the camera-assisted procedure, by analysing the footage of the tests ran at the SUPSI. This analysis shown a difference of about 8% at failure between the true curves from DynaMat experiments determined via strain gauges and the same true curves determined via camera-assisted strain measurements.

Tests at UNICT were ran on identical specimens at similar strain rates and the obtained true curves were compared against those from the SUPSI tests analysed according to the camera-assisted procedure. All the obtained true curves were included in a narrow band showing the equivalence of the two facilities and that this material either is not affected by the strain rate effect or the strain rate effect is small enough to be compared to the scattering of the experimental data. Finally, the equivalent curves obtained with the complete procedure at the SUPSI and at the UNICT were analysed confirming the already shown differences between the true curves.

References

1. Mirone, G., D. Corallo, and R. Barbagallo. "Experimental issues in tensile Hopkinson bar testing and a model of dynamic hardening." International Journal of Impact Engineering 103 (2017): 180-194.
2. Metals Handbook vol8, Metals Park, ASM, 34.1990
3. Montagnani M, Albertini C, Buzzi U, Forlani M. Dispositif de contrainte a accumulation mecanique pour essais dinamique de traction, Institut national de la propriete industrielle–Paris Brevet No. 74.17085. The Patent Office of London, Patent No. 1.473.683; 1974. Italian Patent No. 50008A; 1973
4. Albertini C, Forlani M, Montagnani M, Prosdocimi G, Verheyden N. Dispositif permettant de bloquer e de libèrer brusquement une barre de test soumise à des efforts de traction et/ou de torsion, Brevet Europeen No. O 364919B1; 1992
5. Cadoni, E.; Dotta, M.; Forni, D.; Tesio, N. & Albertini, C. Mechanical behaviour of quenched and self-tempered reinforcing steel in tension under high strain rate Materials & Design, 2013, 49, 657 – 666
6. Bridgman, P.W., Studies in large plastic flow and fracture, Mac Graw-Hill, 1952
7. Mirone G. 2004; A new model for the elastoplastic characterization and the stress–strain determination on the necking section of a tensile specimen. Int J Solids Struct 5(41):3545–64.
8. Verleysen P., Degrieck , Experimental investigation of the deformation of Hopkinson bar specimens J., International Journal of Impact Engineering, 2004. 30: 239–253.
9. Noble J.P., Goldthorpe, B.D., Church, P. Harding, J., The use of the Hopkinson bar to validate constitutive relations at high rates of strain Journal of the Mechanics and Physics of Solids 1999; 47: 1187–1206.
10. Forni D., Chiaia B., Cadoni E., 2016, 'Strain rate behaviour in tension of S355 steel: Base for progressive collapse analysis', Engineering Structures 119: 164 - 173.
11. Asprone D., Cadoni E., Prota A., Manfredi G., 2009, Strain-Rate Sensitivity of a Pultruded E-Glass/Polyester Composite, ASCE - Journal of Composites for Construction 13(6), 558-564.
12. Cadoni E., Dotta M., Forni D., Tesio N., 2015, High strain rate behaviour in tension of steel B500A reinforcing bar', Materials and Structures 48(6), 1803-1813.
13. Forni D., Chiaia B., Cadoni E., 2016, 'High strain rate response of S355 at high temperatures', Materials and Design 94, 467-478.